$m^*=0.066m_e$.[18,19] This value, appropriate to the bottom of the band and zero temperature, would be expected to increase to approximately $0.068m_e$ for the present temperature and carrier concentrations.[18] Thus, a discrepancy exists which, however, may be associated with the small values of $\omega_c\tau$[1,20] No systematic variation in m^* with B (and therefore $\omega_c\tau$) has been observed here, however. It is to be noted that there is general agreement between effective-mass values from Shubnikov–de Haas and other measurements for other materials.

[18] H. Pillar, J. Phys. Soc. Japan Suppl. **21**, 206 (1966).
[19] G. E. Stillman, C. M. Wolfe, and J. O. Dimmock, Solid State Commun. **7**, 921 (1969).
[20] E. N. Adams and T. D. Holstein, J. Phys. Chem. Solids **10**, 254 (1959).

IV. SUMMARY

The existence of Shubnikov–de Haas oscillations in the magnetoresistance of n-type GaAs has been demonstrated for the carrier-density range $2\times10^{16}/\text{cm}^3 < n < 2\times10^{17}/\text{cm}^3$. As with the more widely studied III-V semiconductors, reasonable agreement with theory is obtained for both the field and temperature dependence of the amplitude of the oscillations. From the latter an effective-mass value of $(0.058\pm0.006)m_e$ at $1-2\times10^{17}$ is obtained.

Note added in proof. S. Askenazy, J-P Ulmet, J. Léotin, L. Holan, and A. Laurent have recently reported Shubnikov-de Haas oscillations in an n-type GaAs sample with 4×10^{17} electrons/cm^3 [Solid State Commun. **7**, 717 (1969)].

PHYSICAL REVIEW B VOLUME 1, NUMBER 2 15 JANUARY 1970

Far-Infrared Recombination Emission in n-Ge and p-InSb†

S. N. SALOMON AND H. Y. FAN
Department of Physics, Purdue University, Lafayette, Indiana 47907
(Received 7 August 1969)

Far-infrared recombination emission with wavelengths longer than 90 μ was observed under pulsed conditions from the impact ionization of impurity in n-Ge(Sb) and p-InSb samples at 4.2°K. A fast-response n-InSb free-electron bolometer was used as the detector and various filters were used to isolate the spectral regions. Emission with $h\nu$ near 4 meV is interpreted as recombination of free carriers with the lowest excited state of the impurity for both n-Ge and p-InSb. For the n-Ge sample, emission with $h\nu\sim7.8$ meV is attributed to electron transitions from an excited state to the ground state. There was also some indication of emission with photon energies larger than the ionization energy of 9.7 meV of Sb. For p-InSb, emission was observed at photon energies near the impurity ionization energy of about 7.5 meV. This is attributed to the recombination of free holes with the ground state of the impurity. Under certain conditions of pulse duration and electric field, an afterglow was observed after the electric field was removed from the samples. An explanation is suggested for this phenomenon.

I. INTRODUCTION

FAR-INFRARED radiation of about 100 μ from the recombination of impact-ionized donors in n-type Ge samples doped with Sb and As at 4.2°K was first reported by Koenig and Brown.[1] The signal was detected by observing the photoconductive response of a second sample of Ge which was doped with a donor different from the one used for the generator. The sample was partially broken down by applying a dc voltage. The amount of radiation detected was exceedingly small, about 1.5×10^{-12} W. The radiation was attributed to electrons with kinetic energy of about $10kT$ recombining with the donor ground state or to unreasonably energetic electrons recombining with an excited state of the donor. A second study concerning the recombination radiation of Sb donor in Ge was reported by Ascarelli and Brown.[2] A block of Sb-doped Ge was used as detector. The sample, Ge with smaller Sb doping, was inserted into a hole bored in the detector. A large increase of noise of the detector was observed when an applied electric field produced a breakdown of the sample. The effect was attributed to recombination radiation given by the sample.

The present work on far-infrared emission from impact-ionized n-Ge(Sb) and p-InSb was undertaken to obtain more understanding of the phenomena. The emission, together with the sample conductance, was studied as functions of the applied electric field. Various filters were used to obtain information on the spectrum of emission which facilitates the interpretation in terms of electron transitions. The strongest signals measured involve excited states and they could not have been observed with techniques which are not sensitive for these wavelength regions. The emission from p-InSb was measured for the first time. An afterglow emission

† Work supported in part by a contract from the Advanced Research Projects Agency.
[1] S. H. Koenig and R. D. Brown, III, Phys. Rev. Letters **4**, 170 (1960).
[2] G. Ascarelli and S. C. Brown, Phys. Rev. **120**, 1615 (1960).

was observed which was made possible by operating in pulsed mode. Pulsed operation allowed emission power levels of about 10^{-7} W to be obtained which were about 10^5 times the power levels obtained by Koenig and Brown. A discussion is given on the observed emissions.

II. EXPERIMENTAL TECHNIQUE

A. General

The sample was mounted on a sapphire heat sink placed opposite the detector as shown in the schematic drawing of Fig. 1. Apiezon N-grease provided good thermal contacts between the sample, the sapphire, and the copper fin. In order to provide an additional heat sink for the sample and to keep it firmly pressed against the sapphire, a 0.4-mm crystal quartz plate was placed on top and held in position by a phosphor bronze wire spring whose end was soldered to the copper fin. The quartz plate with its optic axis perpendicular to its face gave a transmission of about 70% for far-infrared radiation. Two leads of insulated copper wire were soldered to the sample. The wires were soldered to a coaxial cable consisting of an insulated wire placed inside a stainless-steel tube. The coax is not shown in the diagram.

The detector was mounted on a copper support. It was insulated with $\frac{1}{4}$-mil Mylar and was held in place with Apiezon N-grease. The copper support was soldered to a stainless-steel tube which had an insulated wire running through it. The detector leads were soldered to the wire and the stainless-steel tube, respectively. The detector and the coax were surrounded by another stainless-steel tube which provided electrical shielding. A small window in front of the detector allowed the infrared radiation to be transmitted. This whole assembly was mounted inside a drilled $\frac{1}{2}$-in. Teflon rod which transmitted far-infrared radiation at about 75% and provided a helium exchange gas chamber for the detector. This way of mounting the detector allowed substantial decoupling of the detector from the outside liquid-helium bath which was necessary on account of the large amount of heat dissipated from the sample.

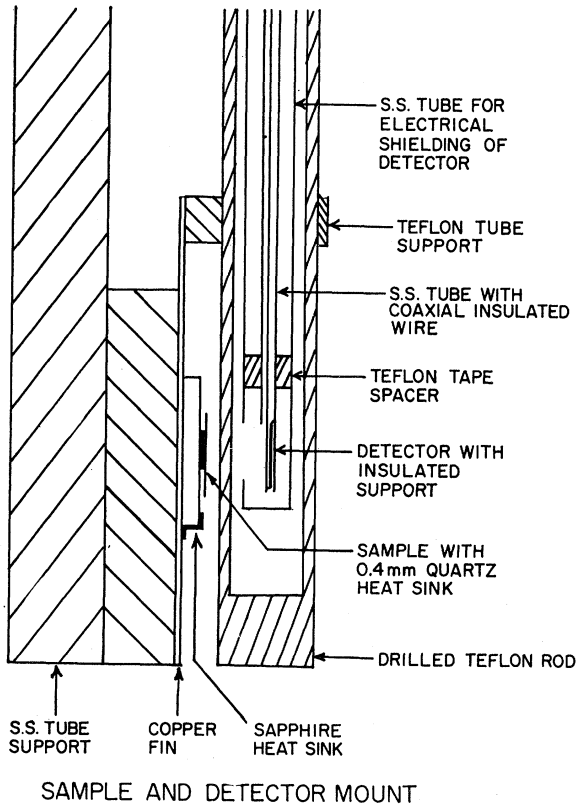

FIG. 1. Schematic diagram of the sample and detector mount.

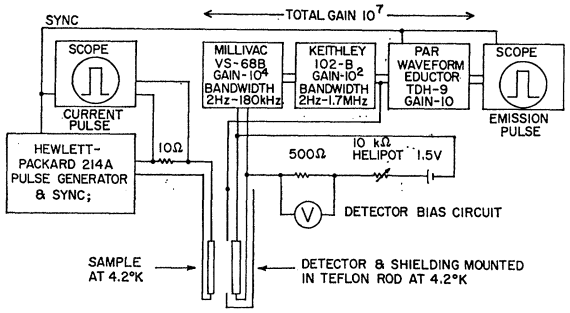

FIG. 2. Schematic diagram of experimental arrangement.

Figure 2 shows the circuit used for pulsing the sample and detecting the far-infrared emission. The generator was internally triggered with a synchronous pulse sent to the oscilloscope and waveform educator. The over-all amplification of the signal was $\sim 10^7$. The waveform educator improved the signal-to-noise ratio by a factor of ~ 500. Conductance measurements were made on the sample by adding two probes to measure the electric field in the sample. The probes were removed for the emission measurements. Most of the measurements were taken with 20-μ sec pulse duration at a repetition rate of 20 pulses/sec.

B. Detector

An n-InSb free-electron bolometer was used to detect the pulsed far-infrared emission from the samples. This type of detector is characterized by its broad band samples. This type of detector is characterized by its broad band spectral response, 60–1000 μ, and fast response time, about 10^{-7} sec. The detector works on the principle that free-carrier absorption raises the energy of electrons giving them a higher mobility. The responsivity, signal per unit incident power, may be written as

$$R = KCA, \qquad (1)$$

where A is the fraction of power absorbed by the detector, C is a parameter which may depend on the wave-

TABLE I. Data of free-electron bolometers discussed in text.

Detector	Detector used, Te-doped	Detectors of Kaplan and Bishop,[a] Se-doped #3	#2	#1
$n(1/cm^3)$:	3×10^{14} ($T=77°K$)	2.3×10^{14}	1.6×10^{14}	7×10^{13} ($T=4.2°K$)
$\mu(cm^2/V\text{-}sec)$; 4.2°K	2.5×10^4	1.33×10^5	1.5×10^5	1.14×10^5
$\sigma(\Omega\text{-}cm)^{-1}$; 4.2°K	1.2	4.9		
Thickness (mm)	0.28	0.3	0.3	0.3
Length (mm)	9.5	8	8	8
Width (mm)	3	3	3	3

[a] See Ref. 3.

length of radiation and the characteristics of the detector material, and K depends on the circuitry. The quantity A is given by the usual formula

$$A=[(1-R)(1-e^{\alpha t})]/(1-Re^{-\alpha t}), \quad (2)$$

where R is the reflectivity, t is the detector thickness, and α is the absorption coefficient. For free-carrier absorption, the classical expression for α is

$$\alpha(\omega)=(4\pi/c\eta)\sigma_0/(1+\omega^2\tau^2), \quad (3)$$

where σ_0 is the static conductivity, η is the refractive index, and τ is the collision time which can be estimated from the mobility of the carriers $\mu=e\tau/m^*$.

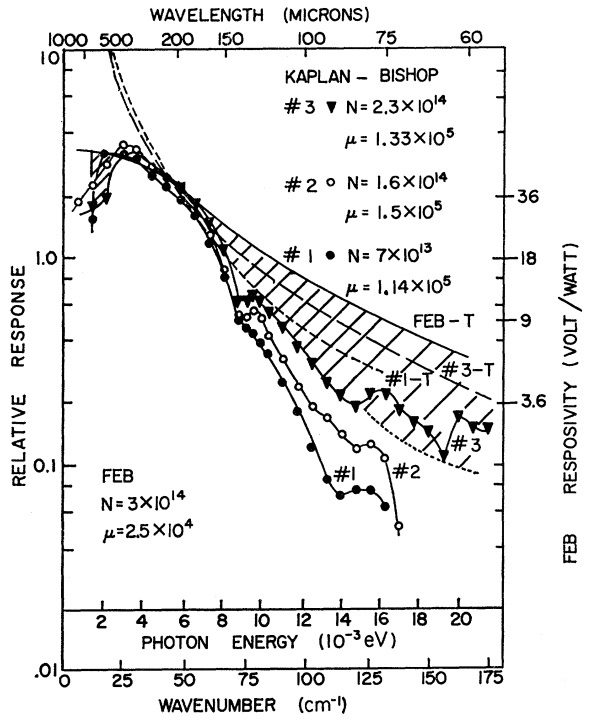

FIG. 3. Response curves of free-electron bolometers relative to that of Golay detector. Curves #1, #2, and #3 are given by Kaplan and Bishop (Ref. 3) for three different bolometers. Curves #1-T, #3-T, and FEB-T are calculated power absorption for the detectors, FEB being the detector used in the present experiment; the curves are normalized to a common point at 200 μ.

Kaplan and Bishop[3] have made a study of such detectors. The relative response curves given for three detectors are shown in Fig. 3 and marked by #1, #2, #3. The curves are given relative to the response of a Golay cell mounted in the spectrometer, i.e., the signal-to-noise ratio of the detector was divided by the signal-to-noise ratio of the Golay. The curves include the effects of the light pipe and polyethylene windows. The latter were responsible for the absorption band at about 73 cm^{-1}. Table I gives the data for the detectors. The dashed curves #1-T and #3-T are the calculated curves of A according to Eq. (3). They are normalized to agree with the experimental curves at 200 μ. The normalizing factor is different for the two curves. The experimental curves are lower at all other wavelengths. Thus, we conclude that the factor C had a maximum at 200 μ and was not a constant for each detector. If the calculated curves were not normalized individually but were multiplied by a single suitable factor, then they would fit approximately the experimental curves for wavelengths less than 100 μ. It appears that the parameter C is independent of wavelength and sample for short wavelengths.

The electrical data for our detector are also given in Table I. The solid curve marked FEB-T is the calculated curve of A for our detector which is normalized to the same point at 200 μ. The absolute value of A of our detector is even larger than that of detector #3, and the curve for our detector lies higher than the curve for detector #3. The curve gives an upper limit corresponding to a constant C equal to its value at 200 μ. The relative response curve for the FEB should lie within the shaded area.

Putley[4] constructed a detector which operated from 200 μ to 2 mm. However, insufficient data were given to make a comparison with the detectors of Kaplan and Bishop and with our detector.

The relative responsivity of our detector system at 200 μ was calibrated by comparing the signal-to-noise ratio with that of each of two Golay detectors. The comparison gave an average value of 1.2 ± 0.3, the signal-to-noise ratio being somewhat different for the

[3] H. Shenker, Naval Research Laboratory Memorandum Report No. 1743, 1967 (unpublished); R. Kaplan, Appl. Opt. 6, 685 (1967).

[4] E. H. Putley, J. Phys. Chem. Solids 22, 241 (1961).

two Golay detectors. According to the specifications of the Golay detectors, the responsivity of our system was 36 ± 13 V/W at 200 μ. The scale of responsivity is given on the right-hand side of Fig. 3. The minimum detectable power was $\sim10^{-9}$ W at 124 μ and $\sim2.5\times10^{-10}$ W at 200 μ.

From the measured power incident on the detector, the radiation intensity at the sample surface can be obtained from the dimensions of the sample and the detector, the separation between the two, and the transmission of intervening walls and filters. The absorption of emitted radiation within the sample is small, and the emission rate per unit volume of the sample can be easily calculated from the radiation intensity at the surface.

C. Filters

Two filters were used in the emission experiments to eliminate visible or short-wavelength infrared radiation: a sheet of Teflon (1.5 mm thick) which showed strong absorption from 8 to 50 μ and a sheet of black polyethylene (0.15 mm thick) which cut out visible- and near-infrared radiation. The transmission curves measured at room temperature are shown in Fig. 4.

TABLE II. Sample data.

Sample	n-Ge (Sb)	p-InSb (undoped)
Carrier concentration (cm^{-3})	1.6×10^{15} (300°K)	6×10^{14} (77°K)
Length (mm)	5.21	5.44
Width (mm)	1.62	2.14
Thickness (mm)	0.21	0.68

Two kinds of filters were used for the isolation of far-infrared emission bands, metal mesh sieves and reststrahlung filters. The two reststrahlung crystals used, TlCl and CsI were obtained from the Harshaw Chemical Co. Plates of the proper thickness, 1 mm for CsI and 1.5 mm for TlCl, were prepared. The transmission characteristics at 4.2°K have been measured by Hadni *et al.*[5,6] and are shown in Fig. 5.

Transmission measurements on three of the mesh filters were made at room temperature up to about 300 μ. The curves are shown in Fig. 5. The curve for mesh #140 from 300 to 380 μ was extrapolated according to the observation of Mitsuishi *et al.*[7] In agreement with these authors, each curve shows a transmission peak at wavelengths equal to about 1.2–1.3 times the mesh constant. The transmission curve for mesh #100 was taken from Mitsuishi *et al.*

[5] A. Hadni, B. Wyncke, P. Strimer, E. DeCamps, and J. Claudel, *Quantum Electronics* (Columbia University Press, New York, 1964), Vol. I, p. 731.

[6] A. Hadni, J. Claudel, E. DeCamps, X. Gerbaux, and P. Strima, Compt. Rend. **255**, 1595 (1962); A. Hadni, J. Claudel, X. Gerbaux, G. Morlot, and J. M. Munier, Appl. Opt. **4**, 487 (1965).

[7] A. Mitsuishi, Y. Otsuka, S. Fujita, and H. Yoshinaga, Japan J. Appl. Phys. **2**, 574 (1963).

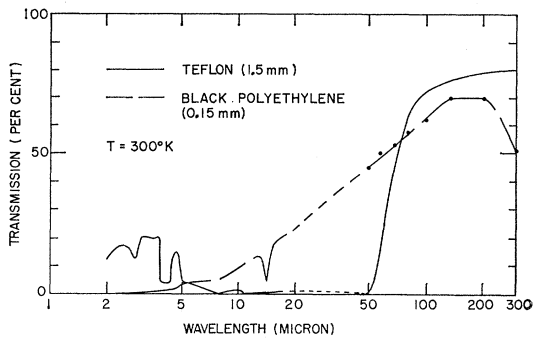

FIG. 4. Transmission curves for Teflon and black polyethylene at room temperature.

III. RESULTS AND DISCUSSION

A. Integrated Intensity

Measurements were made on an Sb-doped n-type Ge and an undoped p-type InSb sample. The data of the samples are given in Table II. Emission measurements were made under applied pulses of 20-μ sec duration with a repetition rate of 20 pulses/sec. The fact that the electrical power supplied to the samples was of the order of tens of watts, whereas the detected power was of the order of nanowatts, leads to the possibility that the detected signal was due to heat radiation. However, the effect of heat radiation was shown to be small from the following estimate. The signal reached a steady-state value after ~4 and ~10 μsec, respectively, in the measurements on the Ge and InSb samples. The rise time was imposed by the circuit and the actual rise time of the signal might have been much shorter. The maximum temperature the sample could have reached in this time may be estimated by assuming that the

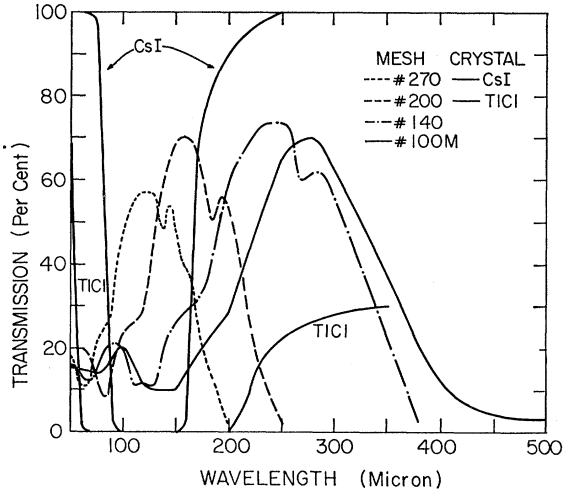

FIG. 5. Transmission curves for wire mesh filters at room temperature and for CsI and TlCl at 4.2°K. The curves for the crystals are taken from Hadni *et al.* (Refs. 5 and 6). The wire mesh curve #100M is from Mitsuishi *et al.* (Ref. 7).

sample was heated adiabatically by the pulse. Specific-heat data are available for Ge[8] and InSb.[9] The spectral emittance of each sample may be obtained from an estimate of the infrared absorption coefficient as a function of wavelength. The upper limit of temperature reached during the signal-rise time was calculated for various power levels of the applied pulse. The heat radiation was calculated corresponding to the upper limits of temperature. The results showed that the contribution of heat radiation should be only a few percent of the steady-state signal detected for all power levels used.

The conductance and emission signal of the germanium sample are shown in Fig. 6 as functions of the pulse field. The conductance rose steeply at about 7.5 V/cm. The emission signal became observable at 12.5 V/cm. With further increase of the field, both the conductance and the emission increased. With a fivefold increase of conductance, the emission signal increased about 25 times. At fields greater than 30 V/cm, the conductance remained constant at $\sigma \sim 12$ $(\Omega\ \text{cm})^{-1}$ and the emission signal increased slowly by at most 37% at 50 V/cm. The large error bars for the three points of emission at highest fields were mainly due to an upward shift in the zero line after the electrical pulse was removed. The top of the error bar corresponds to the emission pulse height measured from the upward shifted zero line which occurred after the electrical pulse was removed from the sample This shift may have been connected with the afterglow discussed later.

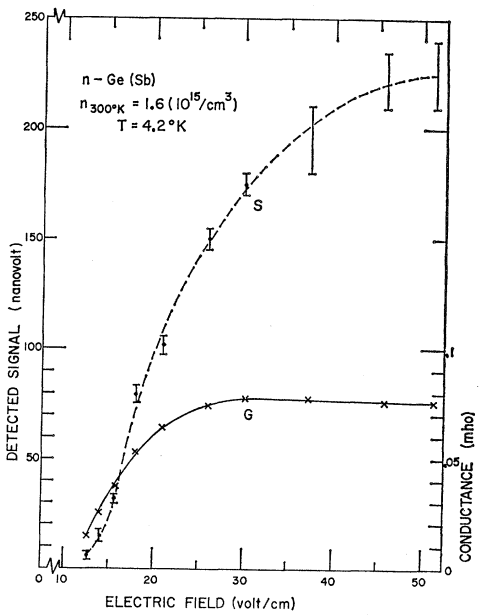

FIG. 6. The far-infared emission signal S and the sample conductance G versus applied electric field for the n-Ge sample at 4.2°K.

[8] P. Flubacher, A. J. Leadbetter, and J. A. Morrison, Phil. Mag. 4, 273 (1959).

[9] T. C. Cetas, C. R. Tilford, and C. A. Swenson, Phys. Rev. 174, 835 (1968).

The behavior of the p-InSb shown in Fig. 7 was qualitatively analogous to that of the n-Ge except at large fields. After a relatively flat region of conductance, there was another sharp increase at about 23 V/cm which was apparently caused by the injection of electron-hole pairs into the sample from the contacts. This explanation was substantiated by probe measurements along the length of the sample and by the observation of emission with photon energies close to the band gap. The far-infrared emission observed with fields larger than 18 V/cm showed a large afterglow after the electrical pulse was removed.

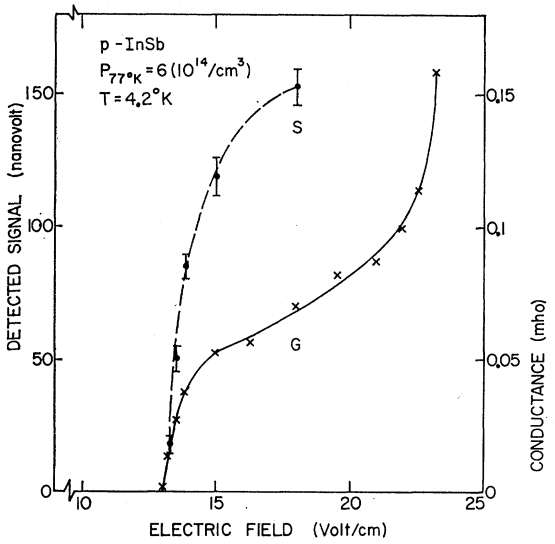

FIG. 7. The far-infrared emission signal S and the sample conductance G versus applied electric field for the p-InSb sample at 4.2°K.

The emission intensity I depends on the product of the density of ionized donors and the density of conduction electrons. When the density of conduction electrons is much greater than the density of compensating acceptors, we have

$$I \propto B(G/\mu)^2, \tag{4}$$

where G is the sample conductance, μ is the electron mobility, and B is the average optical recombination coefficient. For electric fields up to 26 V/cm in n-Ge and 14 V/cm in p-InSb, a linear relationship was found between the emission signal and the square of the conductance, as shown in Fig. 8. It appears that the quantity B/μ^2 was roughly constant for the range of electric field. The emission of the Ge sample increased somewhat at higher electric fields where the conductance was roughly constant, indicating an increase of B/μ^2.

B. Emission Spectra

The spectral distribution of the detected radiation was determined from signals measured with various filters which were inserted between the quartz heat sink and the Teflon tube. The data are listed in Table III. Measurements were made for both directions of applied field. The measured signals were averaged to eliminate the affect of electrical pickup which amounted to $\lesssim 10\%$.

The measurements on Ge were made at a pulsed field of ~ 30 V/cm. Since more than 80% of the signal was transmitted by the Teflon and black polyethylene filters, it must have been due to radiation of wavelengths longer than 50 μ, the wavelength at which Teflon began to transmit. Most of the radiation was concentrated in three spectral regions, as shown by the histogram in Fig. 9.

The band in the 230–360 μ (5.4–3.44 meV) region was deduced primarily from the effect of the # 140 mesh filter used in combination with the TlCl crystal. The TlCl crystal had a short wavelength cutoff at 200 μ and the # 140 filter had a long wavelength cutoff at 380 μ. Together they formed a transparent window with steep sides which peaked at 17% near 280–300 μ. It appears that about 58–65% of the signal was concentrated in the 280–300-μ region. The CsI filter was opaque between 90 and 160 μ and gave a transmission of about 100% at 250 μ. The effect of this filter on the signal shows that at least $32\pm 7\%$ of the signal was in the region 90–250 μ. This is consistent with the estimate that 35–42% of the signal was at wavelengths outside the 230–360-μ region.

The band near 160 μ, about 7.8 meV, was deduced by comparing the data with the CsI crystal in combinations with the mesh filters # 270 and # 200. The CsI with # 270 filter formed a transparent window from 160 to 200 μ with sharp cutoffs; CsI with # 200 filter made a window from 160 to 250 μ with sharp cutoffs, also. For both of these combinations, there was a somewhat less transparent window for wavelengths shorter than 90 μ. However, there was very little radiation for wavelengths less than 90 μ, since large signals were obtained with either of the filters # 270 and # 200 alone. When the filter # 270 in combination with CsI was replaced by # 200, the detected signal increased by a factor of 1.5–2.1. By comparing the transmission windows of the two filters, we conclude that the emis-

TABLE III. Signals measured with various filters are given in terms of signal measured without filters.

Filter	n-Ge (Sb) (%)	p-InSb (%)
# 270	20±3	26±6
# 200	28±4	34±7
# 140	51±6	57±9
CsI	68±7	75±11
CsI # 270	7±2	11±3
CsI # 200	12±2	14±6
TlCl # 270	−1±4	
TlCl # 140	13±2	
Black polyethylene (0.15 mm)	86±10	(≈60)[a]
Teflon (1.5 mm)	84±11	

[a] From an earlier measurement under somewhat different conditions.

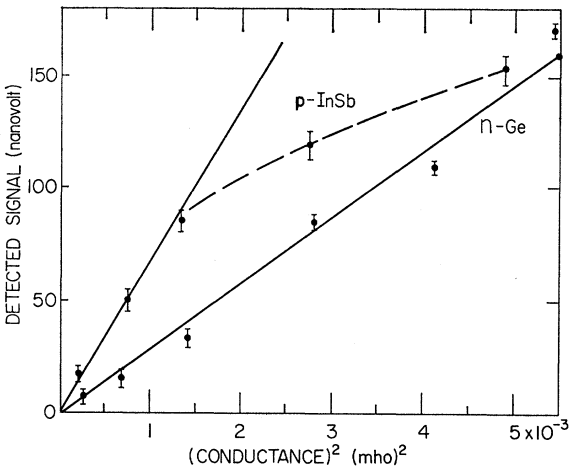

FIG. 8. The far-infrared emission signal versus the square of the sample conductance for applied electric fields up to 26 V/cm for the Ge sample and up to 18 V/cm for the InSb sample.

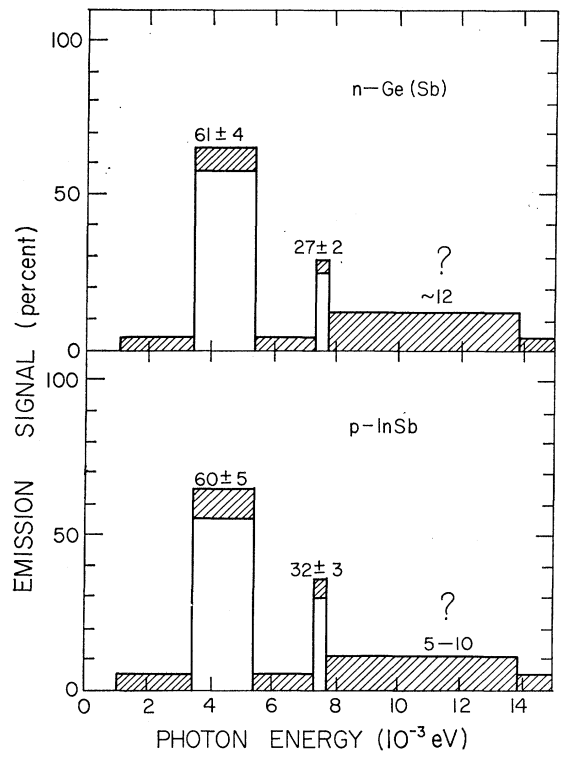

FIG. 9. Histograms of far-infrared emission signal for n-Ge at 30 V/cm and p-InSb at 18 V/cm at 4.2°K. No correction has been made for the spectral responsivity of the detector. The question mark indicates some uncertainty of emission in the high-energy range

sion must have been near 160 μ (where the transmission increased by about 2 times) rather than in the region of 200–230 μ (where the window transmission increased by 10 times or more). There was little radiation from $\sim$170–230μ, and 7.3–5.4 meV.

We deduce with some uncertainty that there was some contribution to the emission signal from the region 90–160 μ. The signal obtained with the #200 filter alone was 1.3–1.5 times higher than the signal obtained with the #270 filter alone. Emission in the region near 160 μ would have caused an increase of 1.5–2.1 times as discussed in the preceding paragraph. This difference which may be questioned on the ground of experimental accuracy indicates that there was some radiation in the short wavelength region where the transmission decreased when the #200 filter was used.

It is interesting to note that when the TlCl crystal was used in combination with the filter #270, the entire far-infrared region for wavelengths greater than 60 μ became opaque. This was in agreement with the experimental observation which gave a negligible signal of $(-1\pm4)\%$.

By the same procedure used for the n-Ge sample, the spectral distribution of the emission from the p-InSb sample was deduced from the measurements listed in Table III. These values were taken at the onset of constant conductance before injection into the sample took place, at an electric field of about 18 V/cm. A histogram of the emission is shown in Fig. 9. It appears to be similar to that of the Ge sample.

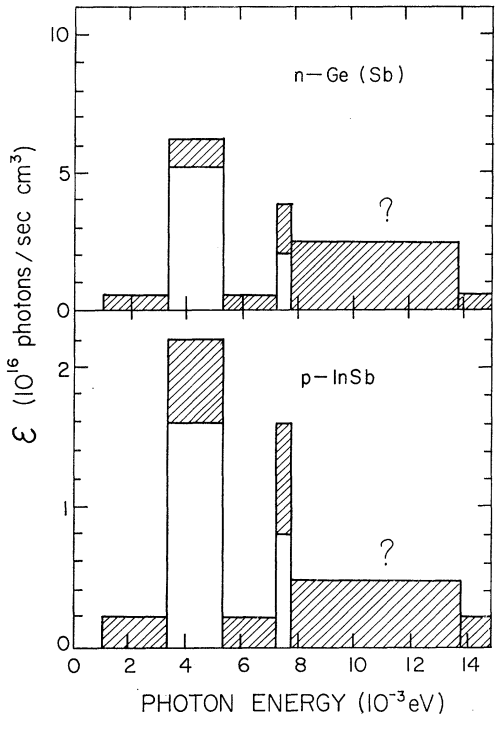

FIG. 10. Histograms of emission intensity for the samples at 4.2°K. The calibration of the intensity scale is good to about a factor of $\approx$2.

Figure 10 shows histograms of emission in photons per second per unit volume of the sample. The histograms were calculated from Fig. 9 using the detector responsivity corresponding to the middle wavelength of each band. The shading represents uncertainties involved in the responsivity and the measurement accuracy. The scale of emission intensity may involve an uncertainty of a factor of 2, being dependent on the detector calibration at 200 μ.

C. Discussion of Emission Spectra

1. Sb-doped Ge

For the Ge sample, recombination of conduction electrons with the ground state of impurity should occur at photon energies exceeding the ionization energy 9.7 meV of Sb. There was indication of emission at such energies though the result involved some uncertainty. The two emission bands at lower energies seen in Fig. 10 must involve excited states of the impurity. The band at lowest energy appears to be given by transitions of conduction electrons to the $(2p,0)$ state which lies $\sim$4.1 meV below the conduction band.[10] The second band at higher energy can be associated with transitions from the $(3p,0)$ state to the ground states which correspond to 7.75 and 7.43 meV, respectively, for the split ground states.

We shall use the hydrogenic model for an estimate of the transitions which involve conduction electrons. An appropriate calculation requires the use of effective mass theory with properly corrected wave functions for the impurity ground state. However, with a value $m^*=0.17m$ consistent with ground-state ionization energy, the hydrogenic model gives for the ground-state absorption cross sections of 1.9×10^{-14} cm^2 for $h\nu=9.7$ meV and 0.86×10^{-14} cm^2 for $h\nu=13$ meV as compared to the respective values of 1.7×10^{-14} and 0.88×10^{-14} cm^2 estimated from the experimental results.[10] Although such comparison can not be made for the excited states for lack of experimental information, it seems that the hydrogenic model may be used for order-of-magnitude estimates.

According to the hydrogenic model, the cross sections of radiative recombination for the $1s$ and $2p$ states are given by[11]

$$\sigma=\eta\left(\frac{m}{m^*}\right)^2\frac{2^7\pi he^2}{3m^2c^3}\frac{E_1}{W}\times\frac{\exp[-4(E_1/W)^{1/2}\operatorname{arctg}(W/E)^{1/2}]}{1-\exp[-2\pi(E_1/W)^{1/2}]}f, \quad (5)$$

[10] J. H. Reuzer and P. Fisher, Phys. Rev. **135**, A1125 (1964).
[11] W. Wessel, Ann. Physik **5**, 611 (1930).

with

$$f_{1s}=(1+W/E_1)^{-2},$$
$$f_{2p}=2(11+12W/E_1)(1+W/E)^{-4},$$

where E_1 is the ionization energy of the $1s$ ground state, E is the ionization energy of the state in question, W is the energy of the conduction electron, and η is the refractive index of the crystal. The rate of photon emission per unit volume is

$$\mathcal{E}=N_i n\int_0^\infty f(W)\sigma v dW\simeq N_i^2\int_0^\infty f(W)\sigma v dW, \quad (6)$$

where N_i is the concentration of ionized impurity, $f(W)$ is the distribution function, and v is the velocity of conduction electrons. For the recombination with the ground states, we take σ to be σ_{1s} given by Eq. (5). For the recombination with the $(2p,0)$ state, we take σ to be $\frac{1}{3}$ of σ_{2p} given by Eq. (5).

The emission measurements were made under conditions where a good part of donors must have been ionized. There is some evidence that with impact-ionization conduction electrons reach an approximate constant concentration of about 0.5 (N_D-N_A)[12,13] in Sb-doped Ge. We have used this value in the approximate estimate of emission intensity. The conduction electrons are assumed to have Maxwell-Boltzmann distributions corresponding to a temperature T_e. Calculation has been made for two values of T_e, 30 and 80°K. According to Conwell,[14] it is reasonable to take T_e to be the crystal temperature 30°K at which approximately one-half of the impurities are thermally ionized. The high value, $T_e=80$°K, corresponds to a mean electron energy equal to the ionization energy of the impurity; Koenig *et al.*[12] assumed the mean electron energy to be of this order of magnitude. The contribution to the integral (6) drops rapidly with increasing W. The integration was carried out to $W\sim E_1$. About 90% of the total comes from $W<0.5E_1$.

The calculated rate of photon emission per unit time for the transition of conduction electron to $(2p,0)$ state is

$$\mathcal{E}=4.2\times10^{16}\ \text{sec}^{-1}\ \text{cm}^{-3}, \quad \text{for } T_e=30°\text{K}$$
$$\mathcal{E}=1.4\times10^{16}\ \text{sec}^{-1}\ \text{cm}^{-3}, \quad \text{for } T_e=80°\text{K}.$$

This compares satisfactorily with the experimental values of $\mathcal{E}\sim5.3\times10^{16}$ sec^{-1} cm^{-3} ($\sim6\times10^{-8}$ W for the sample) for the band of lowest photon energy. As pointed out before, the experimental value is subject to the uncertainty in the calibration of the detector at 200 μ. The experimental result corresponds to an average cross section for recombination of $\bar{\sigma}=5\times10^{-21}$ and 8×10^{-21} cm^2, for $T_e=30$ and 80°K, respectively.

For the transition of conduction electrons to the ground states, the calculation gives

$$\mathcal{E}=3.9\times10^{17}\ \text{sec}^{-1}\ \text{cm}^{-3}, \quad \text{for } T_e=30°\text{K}$$
$$\mathcal{E}=1.2\times10^{17}\ \text{sec}^{-1}\ \text{cm}^{-3}, \quad \text{for } T_e=80°\text{K}.$$

Experimentally, the indication is that radiation with $h\nu>E_1$ could have been present with $\mathcal{E}\sim0.25\times10^{17}$ sec^{-1} cm^{-3} (6×10^{-8} W for the sample), corresponding to $\bar{\sigma}\sim2\times10^{-21}$ cm^2. With the uncertainty of detector calibration taken into account, a maximum possible value is estimated to be 0.4×10^{17} sec^{-1} cm^{-3}, which is considerably lower than the calculated value. It seems that better calculation or measurement with better sensitivity at the high photon energies is necessary to resolve the discrepancy.

Consider now the central emission band around 7.5 meV of photon energy. It has been attributed to transitions of Sb from the $(3p,0)$ excited state to the ground state. The Einstein coefficient A, for the rate of transition may be estimated from the expression

$$A=\frac{8\pi\eta^2\nu^2 g_o}{Nc^2 g_e}\int\alpha(\nu)d\nu,$$

where the subscripts o and e refer to the ground state and the excited states, respectively, g is the degeneracy of the state, N is the impurity concentration, and $\alpha(\nu)$ is the absorption coefficient associated with transitions from the ground state to the excited state. The rate of photon emission is given by $\mathcal{E}=N_eA$, N_e being the concentration of impurity in the excited state. Using the data on the integrated absorption, we get from the measured emission rate a value of $N_e/N\sim50\%$, which appears high.

Emission from Sb and from As in Ge was reported by Koenig and Brown.[1] The signal was detected by the photoresponse of a second piece of Ge doped with the other impurity. Both the sample and the detector were enclosed in a cavity so that most of the emitted photons reached the detector. Impact ionization was produced by dc voltage and the level of ionization was low. For the Sb-doped sample with $N_D-N_A=2.2\times10^{14}$ cm^{-3}, an emission rate of $\sim10^9$ photons/sec was obtained, which gave an average recombination cross section of $\sim10^{-22}$ cm^2. A later work[12] gave a better estimate of the thermal ionization coefficient for the impurity of the detector which indicated that these numbers ought to be seven times larger. A value of $\sim10^{-22}$ cm^2 was thought to be reasonable in the light of the hydrogenic models of Lampert[15] and Burstein *et al.*[16] We estimate that the

[12] S. H. Koenig, R. D. Brown, III, and W. Schillinger, Phys. Rev. **128**, 1668 (1962).

[13] E. J. Ryder, I. M. Ross, and D. A. Kleinman, Phys. Rev. **95**, 1342 (1954).

[14] E. M. Conwell, *High Field Transport in Semiconductors* (Academic Press Inc., New York, 1967), p. 146.

[15] Lampert was quoted by S. H. Koenig and R. D. Brown in Ref. 1, R. Braunstein, M. A. Lampert, E. G. Linder, RCA Laboratories, Signal Corps Project No. 27-322-B, Contract No. DA36-039-5548, Eleventh Quarterly Report, 1954 (unpublished). This report may be obtained from the Defense Documentation Service AD 41325. The reference to this unpublished work was kindly supplied by S. H. Koenig.

[16] E. Burstein, J. S. Picus, and N. Scalar, in *Proceedings of the Conference on Photoconductivity, Atlantic City, 1954*, edited by R. G. Breckenridge *et al.*, (John Wiley & Sons, Inc., New York, 1956), p. 353.

concentration of electrons produced by impact ionization was $n\sim3\times10^{12}$ cm^{-3}, from the given data on conductivity. Assuming T_e to be in the range 20°K to 100°K, we calculate from Eq. (6) an emission rate of $\sim2\times10^{11}$ photons/sec which corresponds to an average recombination cross section of $\sim10^{-20}$ cm^2. The lower limit of integration is taken to be $W=3$ meV instead of $W=0$, in order to take into account that the ionization energy of As in the detector is higher by ~3 meV than that of the Sb impurity in the sample. It is seen that the experimental result of Koenig and Brown appears to be too low in comparison with the calculated value. The situation is analogous to that found in our results concerning conduction electron to ground state transitions.

2. p-InSb

The material was not intentionally doped. From photoluminescence measurements, an impurity-ionization energy was estimated to be 7.5±0.5 meV. The residual acceptors were probably either Zn or Cd. As shown in Fig. 10, there was indication of emission with $h\nu\gtrsim7.8$ meV. Such emission could be given by transitions of free holes to the ground state of impurity. Using $m_h\sim0.4m$, an average radiative recombination cross section was estimated to be $\approx2\times10^{-20}$ cm^2 which is significantly larger than that estimated for the ground state of Sb in the Ge sample.

The valence band structure of the III-V compounds is rather similar to that of Ge and Si except for the fact that there are band maxima not exactly at $k=0$. From cyclotron resonance measurements,[17,18] the light hole mass of InSb is about twice that of Ge, but the heavy hole masses of the two materials are about the same. Assuming that the excitation spectrum of acceptors in InSb is roughly the same as that in Ge, the emission band of lowest energy can be interpreted as recombination of free holes with the lowest excited state. It could also be attributed to transitions from an excited state to the ground state. Under the assumption that the emission is given by free hole to excited state transitions, the average radiative recombination cross section was calculated to be $\approx3\times10^{-20}$ cm^2 for an intensity of $\approx2\times10^{16}$ photons/sec cm^3 ($\approx10^{-7}$ W from the sample).

D. Afterglow

1. n-Ge

Several examples of the detected signal as a function of time are shown in Fig. 11. An electric field of 30 V/cm and a pulse repetition rate of 20 pulses/sec were used. Figures 11(a), 11(c), and 11(d) were taken with the output filter smoother which connects the channels of the waveform educator. Figure 11(b) was taken without the smoother and discrete channels of 1 μsec width are evident.

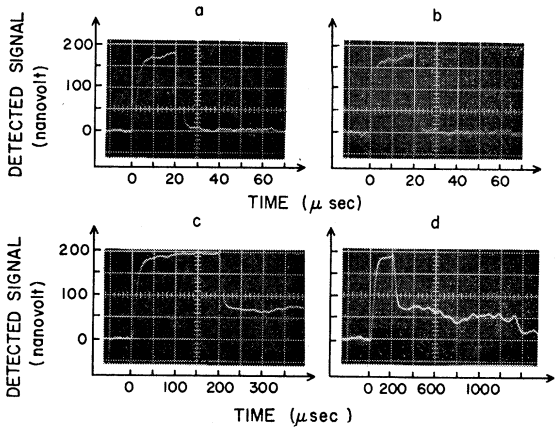

FIG. 11. Oscilloscope photographs of the detected signal for the Ge sample at 4.2°K. (a) 20-μsec pulse with smoother, (b) 20-μsec pulse without smoother, (c) and (d) 200-μsec pulse with smoothed channels of 5 μsec and 20 6sec widths, respectively.

Figure 11(b) shows that the detected signal reached a maximum amplitude of about 175 nV within 2–4 μsec; the signal was fairly flat. After the pulse was removed, the signal decayed to about zero within 2–4 μsec. The rise and fall times of the signal corresponded to the frequency response of the detector electronics. The actual rise and fall times of light emission might have been much faster, being limited by the nonradiative recombination rate. The measured rise and fall times of the applied voltage and the current in the sample were about 0.1 μsec, which might have been circuit limited also.

When the pulse duration was extended to 200 μsec, the magnitude of the signal remained about constant. This is shown in Fig. 11(c). Contrasted to the 20-μsec electrical pulse which was flat to about 3%, the 200 μsec pulse was not, i.e., the current decreased by about 10% and the field increased by about 37% during the length of each pulse. This deviation from flatness was probably due to sample heating. However, the fact that the emission signal increased only a small amount over such a long duration, from 4 to 200 μsec, is supporting evidence that the contribution of heat radiation to the observed signal was negligible. After the pulse was switched off, the signal did not return to zero immediately as in the 20 μsec case, but dropped to about 70 nV where it decayed very slowly as a function of time. This effect is shown clearly in Fig. 11(d). The smoothed channel width was 20 μsec, which accounted for the apparent slow rise and fall times. The afterglow signal approached zero more than 2000 μsec after the electrical pulse was removed.

By means of an electrical probing pulse supplied by a second pulse generator, the conductance of the sample was measured during the afterglow period. The probe electric field of 10-μsec duration was sufficiently small,

[17] D. M. S. Baggauley, M. L. A. Robinson, and R. A. Stradling, Phys. Letters **6**, 143 (1963).

[18] H. T. Tohver and G. Ascarelli, in *Proceedings of the Ninth International Conference on the Physics of Semiconductors, Moscow, 1968* (NAUKA, Leningrad, 1968), p. 326.

<0.2 V/cm, so that it produced little impact ionization. The results showed that the conductance after the removal of the 200-μsec pulse was approximately one-half the breakdown conductance. It decreased rather slowly, by 75% after 3.5 msec.

Some filter measurements were made in order to determine the range of wavelength of the afterglow. It was found that the effect of various filters, CsI, #200, #270, on the signal at 100 μsec after pulse removal was rather similar to the effect observed during the pulse. It appeared that the transitions producing the afterglow were in general similar to those which produced the ratiation when the field was applied. A possible difference could come from the fact that the electrons were hot when the field was applied and were more thermalized after the removal of the field. The fact that the afterglow appeared for the 200-μsec pulse whereas there was no discernible afterglow for the 20-μsec pulse can be understood on the basis that a higher lattice temperature was reached with the longer pulse and a larger fraction of the donors was kept ionized.

2. *p-InSb*

The detected emission signals for a 200-μsec pulse duration are shown by the photographs of Fig. 12 for two different electric fields. Figure 12(a) shows that the signal dropped to almost zero when the pulse was removed. Presumably, the applied field was sufficient to impact ionize the acceptors but was low enough so that there was little injection of electron-hole pairs from the contacts. The conductance measured at 100 μsec after removal of the breakdown pulse was 5% of the conductance during the pulse. At the high pulse field $E\sim 23$ V/cm, strong injection was indicated by the conductance measurements; at 100 μsec after the removal of the pulse, the conductance was still as high as 25% of the conductance during the pulse. The power input to the sample increased several times. With applied pulses of this magnitude, a strong afterglow appeared after removal of the pulse as shown in Fig. 12(b). The two spikes at 0 and 200 μsec were due to electrical pickup, these results being taken from early measurements where the pickup was more severe. The increase in the emission signal by about 25% with current kept constant might have been associated with the fact that the voltage across the sample increased by 10% over the duration of the pulse. Figure 12 (c) shows that the afterglow took about 8 msec to decay.

Near-band-gap radiation due to the recombination of injected electron-hole pairs was observed while the

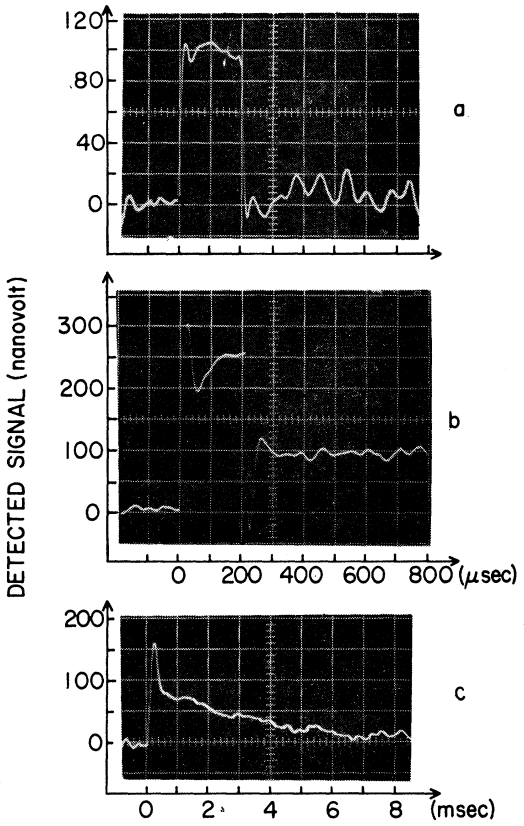

FIG. 12. Oscilloscope photographs of the detected signal for the p-InSb sample at 4.2°K, taken with 200-μsec pulses; (a) with $E\sim 18$ V/cm, no injection of hole-electron pairs; (b) and (c) with $E\sim 23$ V/cm, strong injection; (a) and (b) were taken with smoothed channels of 10 μsec width; and (c) was taken with a channel width of 100 μsec.

electrical pulse was applied to the sample. In order to rule out the possibility that the afterglow was due to near-band-gap radiation, a measurement was made with black polyethylene as a filter, which is opaque in the near infrared. The filter only reduced the signal to 60% showing that the afterglow must have been due to long-wavelength radiation as for the n-Ge sample. The cause of the afterglow appeared to be that the sample temperature was raised by the pulse and the conductance after removal of the pulse was due to free holes generated by thermal ionization. The injected carriers should have recombined very rapidly. The afterglow lasted a longer time in the p-InSb sample than in the Ge sample because the former was about three times thicker and its heat capacity was larger.

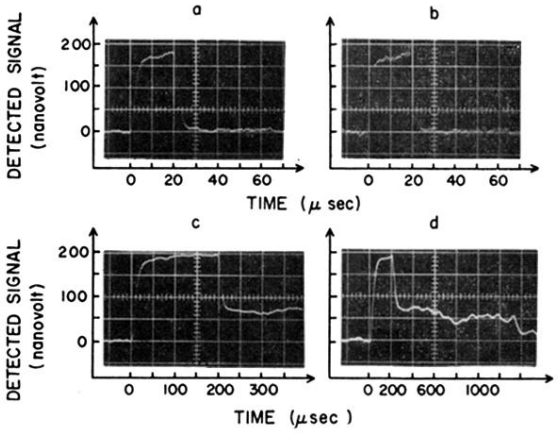

FIG. 11. Oscilloscope photographs of the detected signal for the Ge sample at 4.2°K. (a) 20-μsec pulse with smoother, (b) 20-μsec pulse without smoother, (c) and (d) 200-μsec pulse with smoothed channels of 5 μsec and 20 6sec widths, respectively.

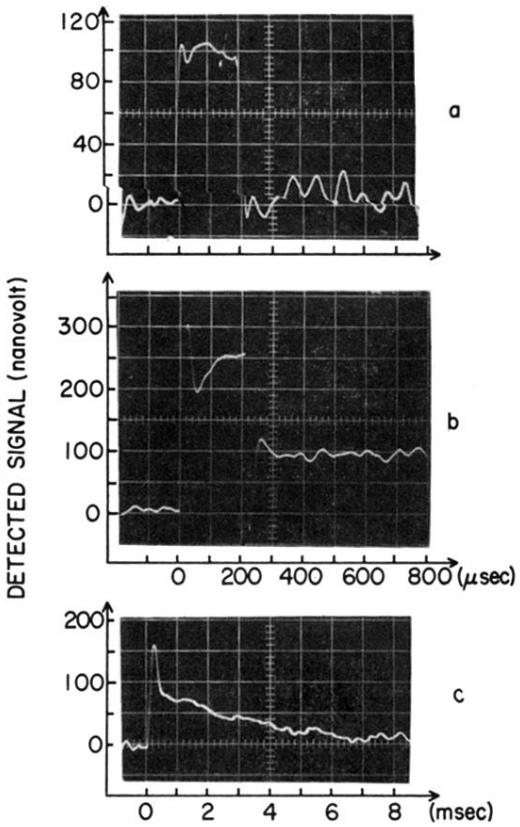

FIG. 12. Oscilloscope photographs of the detected signal for the p-InSb sample at 4.2°K, taken with 200-μsec pulses; (a) with $E\sim 18$ V/cm, no injection of hole-electron pairs; (b) and (c) with $E\sim 23$ V/cm, strong injection; (a) and (b) were taken with smoothed channels of 10 μsec width; and (c) was taken with a channel width of 100 μsec.